Hindawi Publishing Corporation
International Journal of Photoenergy
Volume 2014, Article ID 846581, 6 pages
http://dx.doi.org/10.1155/2014/846581

Research Article

Ultrathin Anode Buffer Layer for Enhancing Performance of Polymer Solar Cells

Dun Wang,[1] Jian Wang,[1] Ling-liang Li,[1] Qiao-shi An,[1] Hui Huang,[2] Chao-qun Jiao,[2] Yang Liu,[1] and Fu-jun Zhang[1]

[1] *Key Laboratory of Luminescence and Optical Information, Ministry of Education, Beijing Jiaotong University, Beijing 100044,China*
[2] *School of Electrical Engineering, Beijing Jiaotong University, Beijing 100044, China*

Correspondence should be addressed to Fu-jun Zhang; fjzhang@bjtu.edu.cn

Received 23 April 2014; Accepted 11 May 2014; Published 28 May 2014

Academic Editor: Dewei Zhao

A series of polymer solar cells (PSCs) based on poly[(4,8-bis-(2-ethylhexyloxy)-benzo[1,2-b:4,5-b′(dithiophene)-2,6-diyl-alt-(4-(2-ethylhexanoyl)-thieno[3,4-b]thiophene)-2,6-diyl] (PBDTTT-C) and [6,6]phenyl-C71-butyric acid methyl ester ($PC_{71}BM$) were fabricated with various anode buffer layers. The power conversion efficiency (PCE) of PSCs was improved to 4.91% for the cells with PEDOT:PSS/LiF (1 nm) as anode buffer layer, which corresponds to 26.2% efficiency improvement compared with the cells with PEDOT:PSS as anode buffer layer. The PSCs with PEDOT:PSS/LiF as anode buffer layer show a maximum short-circuit density (J_{sc}) of 13.70 mA/cm^2, with open circuit voltage (V_{oc}) of 0.73 V and fill factor (FF) of 49.1% under illumination 100 mW/cm^2 AM 1.5 G simulated solar light. The dominant mechanism for the performance improvement of PSCs could be attributed to the increased charge carrier collection ability by anode buffer layers.

1. Introduction

In the past ten years, as the demand for renewable energy becomes more and more urgent, polymer solar cells (PSCs) have been considered as next generation photovoltaic devices to solve energy crisis due to its many advantages, such as flexibility, light weight, environmental friendly, and easy large-area applications [1]. Many strategies have been introduced on improving the power conversion efficiency (PCE) and stability of PSCs, such as the development of novel donor and acceptor materials [2], the novel processing approaches to induce optimal microstructures in the active layer [3], and the optimization of interfacial buffer layer for efficient charge carriers collection [4]. The PCE of PSCs has been improved to more than 6% with a narrow band gap polymer poly[(4,8-bis-(2-ethylhexyloxy)-benzo[1,2-b:4,5-b′]dithiophene)-2,6-diyl-alt-(4-(2-ethylhexanoyl)-thieno[3,4-b]thiophene)-2,6-diyl] (PBDTTT-C). The key requirement for efficient operation of all-organic electronic devices is the process of the charge carriers injection and collection between active layer and electrodes. Therefore, the optimization of interfacial buffer layer is required to form ohmic contact for better charge carriers collection, resulting in increased short-circuit current density (J_{sc}) and fill factor (FF) of PSCs.

It is known that anode buffer layer plays an important role in determining the performance of organic light emitting diodes (OLEDs) and the PSCs. The operation mechanism of anode buffer layer is more complex in real PSCs. The main mechanism can be summarized as follows: (i) to adjust the effective work function of the electrode [5], (ii) to realize a vacuum level offset between the active layer and the electrode by forming a dipole layer [6], (iii) to increase built-in electric field by forming a tunneling junction [7], and (iv) to protect organic active layer from the hot electrode atoms during thermal deposition [8]. Helander et al. reported that the alkali halide (typically LiF in combination with an Al cathode) inserted between electrodes and the active layer can form a dipolar salt layer, then reducing the electron-injection barriers or extraction losses in the PSCs [9, 10]. As we know, poly(3,4-ethylenedioxythiophene):poly(styrenesulfonate) (PEDOT:PSS) is commonly

used as anode buffer layer to enhance J_{sc} as well as open circuit voltage (V_{oc}) for PSCs. PEDOT:PSS consists of PSS, which has hygroscopic and acidic characteristics. The PSS can corrode ITO and set off chemical reaction with the active layer materials, which degrades the cell performance [11]. In order to solve this problem, the metal oxides of zinc oxide (ZnO) [12], nickel oxide (NiO) [13], molybdenum oxide (MoO_3) [14, 15], and tungsten oxide (WO_3) [16] have been demonstrated as an effective replacement of PEDOT:PSS to improve the stability of PSCs. However, it is difficult to control the work function of the metal oxides for desired applications [17]. Recently, Chen et al. reported that solution-processed MoO_3 doped into PEDOT:PSS extends the interfacial contact area between the active layer and PEDOT:PSS layer, which facilitates hole collection at the anode; the performance and stability of the PSCs were improved [18]. In this paper, we reported the effects of PEDOT:PSS/LiF as anode buffer layer on the performance of PSCs. The PCE of PSCs was improved to 4.91% with a PEDOT:PSS/LiF (1 nm) double anode buffer layer system, which leads to a significant efficiency improvement of about 26.2% compared with a single PEDOT:PSS buffer layer. The optimized PSCs have J_{sc} of 13.70 mA/cm^2, with V_{oc} of 0.73 V and FF of 49.1% under illumination 100 mW/cm^2 AM 1.5 G simulated solar light.

2. Experimental Section

The indium tin oxide (ITO) glass substrates with sheet resistance 15 Ω/□ were cleaned continuously in ultrasonic baths containing acetone, detergent, deionized water, and ethanol. Then the cleaned ITO substrates were blow-dried by high pure nitrogen gas and then treated by UV-ozone for 10 minutes to increase the work function of ITO. The solution of PEDOT:PSS (Clevios PVP Al 4083, purchased from H.C. Starck co. Ltd.) was spin-coated onto the cleaned ITO substrates under 5000 rounds per minute (RPM) for 40 s to fabricate the interfacial layers. Then PEDOT:PSS coated ITO glass substrates were annealed in air at 120°C. After drying for 10 minutes, the substrates were transferred to a nitrogen-filled glove box. The polymer material PBDTTT-C (Product number: SMI-P9001, purchased from Solarmer Energy, Inc.) and [6,6]phenyl-C_{71}-butyric acid methyl ester ($PC_{71}BM$) (Product number: LT-S923, purchased from Luminescence Technology Corp) with a weight ratio of 1 : 1.5 were dissolved in 1,2-dichlorobenzene at a concentration of 25 mg/mL. The blend solution was stirred by a magnetic stirrer at 27°C for 24 hours; then the active layers were fabricated by spin-coating method at rate of 1400 RPM in a high purity nitrogen filled glove box. The 1 nm LiF interfacial layer and about 100 nm cathode layer Al were deposited by thermal evaporation under 10^{-4} Pa vacuum conditions, and the thickness was monitored by a quartz crystal microbalance. The active area of about 3.8 mm^2 is defined by the vertical overlap of ITO anode and Al cathode. The cell architecture is ITO/buffer layer/PBDTTT-C:$PC_{71}BM$/LiF/Al. For convenient comparison, the PSCs with various anode buffer layers were marked by Cells A to D:

Cells A: Glass/ITO/PBDTTT-C:$PC_{71}BM$/LiF/Al,

Cells B: Glass/ITO/LiF (1 nm)/PBDTTT-C:$PC_{71}BM$/LiF/Al,

Cells C: Glass/ITO/PEDOT:PSS/PBDTTT-C:$PC_{71}BM$/LiF/Al,

Cells D: Glass/ITO/PEDOT:PSS/LiF (1 nm)/PBDTTT-C:PC_{71} BM/LiF/Al.

The absorption spectra of films were measured with a Shimadzu UV-3101 PC spectrophotometer. The current density-voltage (J-V) characteristics of the PSCs were measured using a Keithley 4200 source measurement unit and an ABET Sun 2000 solar simulator at room temperature in air. The external quantum efficiency (EQE) spectra were measured by a Zolix Solar Cell Scan 100. The schematic architecture of the PSCs, the molecular structures of PBDTTT-C and $PC_{71}BM$, and the energy level structure are shown in Figure 1.

3. Results and Discussion

The normalized absorption spectra of pure PBDTTT-C and $PC_{71}BM$ films and their blend films (1 : 1.5) were measured and are shown in Figure 2. It is apparent thatpure PBDTTT-C films show a relatively strong absorption in the range from 600 nm to 750 nm and a relative weak absorption in the shorter wavelength range from 350 nm to 600 nm. The main absorption peak of PBDTTT-C locates at 700 nm. The highest occupied molecular orbital (HOMO) and the lowest unoccupied molecular orbital (LUMO) levels of PBDTTT-C are 5.12 eV and 3.35 eV, with the band gap of about 1.77 eV according to the absorption peak at about 700 nm [19]. There are two apparent absorption peaks at 375 nm and 480 nm for pure $PC_{71}BM$ films, which could broaden light absorption range of the blend films. Therefore, the normalized absorption spectrum of blend films shows two distinct absorption peaks at 460 nm and 700 nm, resulting from their absorption spectral overlap. Based on the PBDTTT-C:$PC_{71}BM$ as the active layers, a series of PSCs with various anode buffer layers were fabricated and measured under the same conditions.

The current density-voltage (J-V) characteristic curves of PSCs were measured under dark conditions and are shown in Figure 3(a). It is apparent that Cells B, C, and D with anode buffer layers have lower leak current densities under reverse bias, compared with that of Cells A prepared on bare ITO substrates. This indicates that anode buffer layers could improve the interface between the ITO anode and the active layer. Cells D with PEDOT:PSS/LiF as anode buffer layer show the best diode quality with lower leak current density and high rectification ratio; the rectification ratio $|J(1v)|/|J(-1v)|$ is as high as ~10^4.

The J-V characteristic curves of PSCs with various anode buffer layers were measured under illumination 100 mW/cm^2 AM 1.5 G simulated solar light and are shown in Figure 3(b). The key parameters of PSCs are summarized in Table 1. It is apparent that Cells D have relatively larger V_{oc} than those of Cells A and B, and the V_{oc} of Cells D remain almost the same compared with that of Cells C. As we know V_{oc} of PSCs is primarily determined by two factors: (i) the energy levels difference between the HOMO

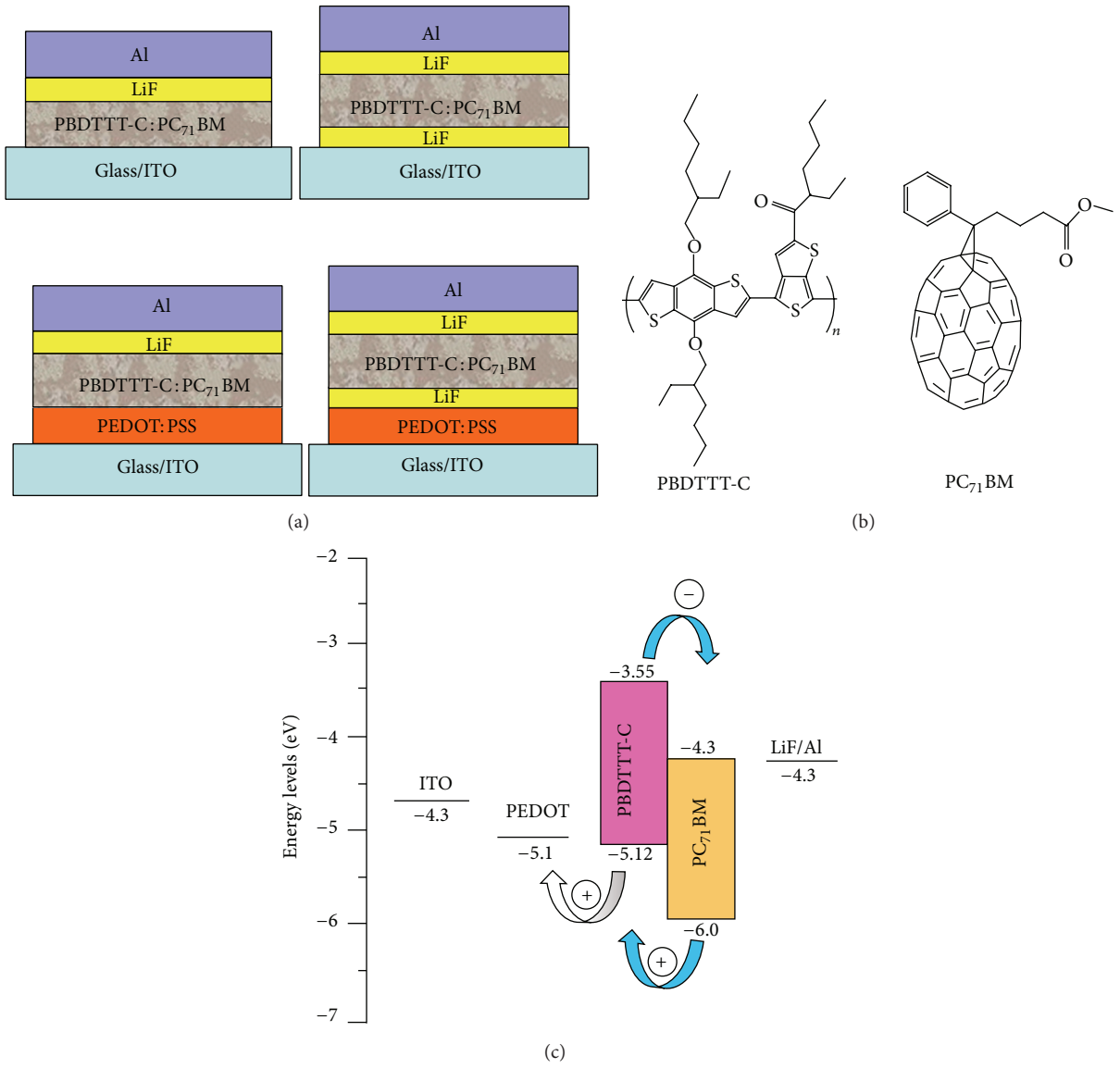

FIGURE 1: (a) The schematic architecture of the PSCs. (b) Molecular structure of PBDTTT-C and $PC_{71}BM$. (c) The energy level structure of materials.

of the electron donor and the LUMO of electron acceptor and (ii) the work function difference between anode and cathode electrode [20]. It could be assumed that the improved V_{oc} of Cells D was due to the changes of anode work function since the active layer fabrication condition and the cathode layer deposition remain constant. The work function of PEDOT:PSS (5.1 eV) is 0.4 eV higher than that of ITO (4.7 eV). The PEDOT:PSS layer can effectively tune the work function of ITO substrates for Cells C and D. According to the V_{oc} of Cells C and D, the thin LiF layer may have no obvious effect on the work function of ITO substrates. It is worthwhile to mention that the J_{sc} of Cells D is 13.70 mA/cm^2, which is a 14.4% increase compared with that of Cells C. The increase of J_{sc} could be attributed to the enhancement of holes extraction efficiency by the ultrathin anode buffer layer. It is known that PEDOT:PSS is conductive polymer with high ductility, which could be considered as a kind of metal. The metal-insulator-semiconductor (MIS) model could be formed, which is based on PEDOT:PSS/LiF/organic active layer, because LiF and organic active layer materials are commonly considered as insulator and semiconductor, respectively. As reported by Xi et al. when the generated holes in the active layer come to the interface of LiF/organic active layer, a large number of them will pass through the ultrathin LiF layer by the tunneling [21]. The FF of Cells D is increased about 10.3% compared with that of Cells C. This may be due to the improved interfacial contact between the active layer and PEDOT:PSS layer due to the insertion of a thin LiF layer. Kim and Chang reported that a thin LiF layer evaporated onto PEDOT:PSS layer could reduce film roughness, which shows smooth surface morphology of the anode buffer layer [22]. It is known that the shunt resistance (R_{sh}) and series

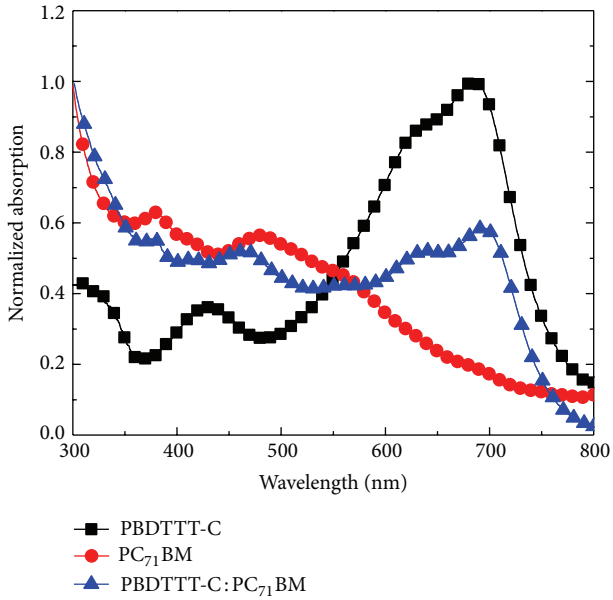

Figure 2: Normalized absorption spectra of PBDTTT-C, $PC_{71}BM$, and their blend films with 1 : 1.5 weight ratio.

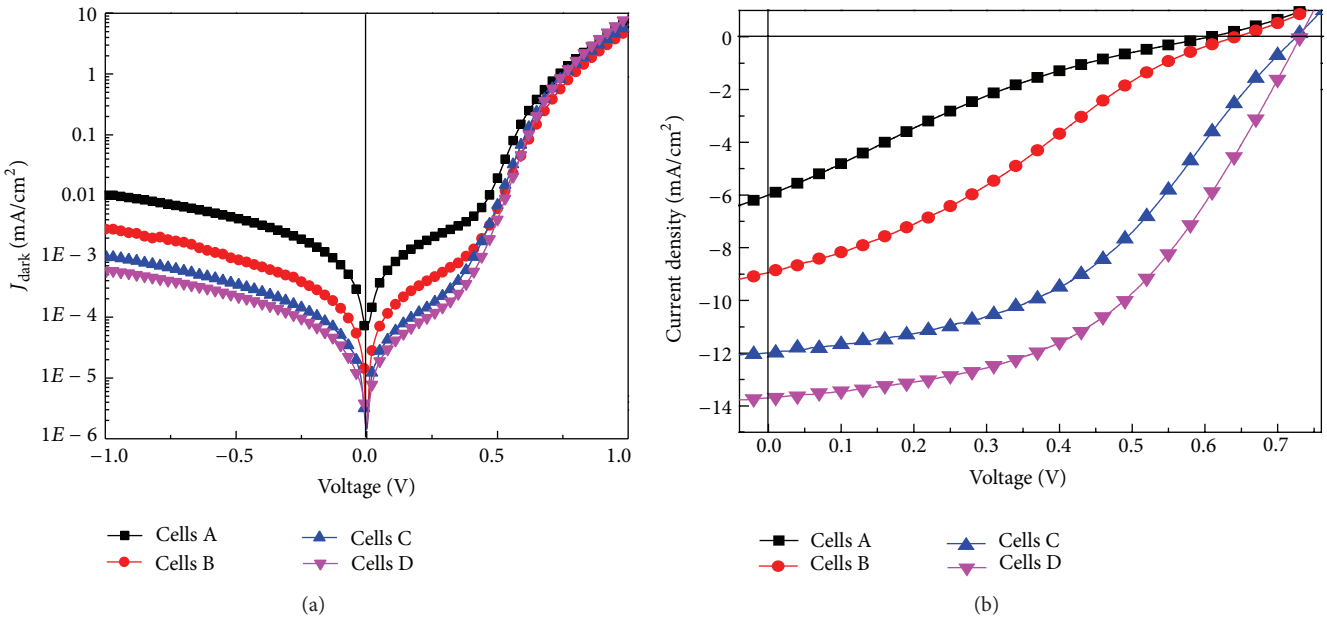

Figure 3: (a) Single logarithmic of *J-V* characteristics curves of PSCs with various anode buffer layers in dark conditions. (b) *J-V* characteristics curves of PSCs with various anode buffer layers under illumination 100 mW/cm^2 AM 1.5 G simulated solar light.

resistance (R_s) are two important parameters in the PSCs. In contrast to Cells C, the R_{sh} of Cells D was increased about 19% and the R_s was decreased about 44% due to the insertion of a thin LiF layer. The R_{sh} is generally associated with leakage current which is determined by the film quality and its interfaces. Small R_{sh} results from the loss of charge carriers through leakage paths including pinholes in the films and the recombination and trapping of the carriers during their transit through the active layer [23]. The R_s is mainly related to the contact resistance between the active layer and anode electrode. The decrease of R_s of Cells D should be attributed to the formation of a better ohmic contact due to the insertion of a thin LiF layer.

In order to further clarify the effect of the LiF interlayer on performance of the PSCs, the external quantum efficiency (EQE) spectra of Cells C and D are investigated and shown in Figure 4. It is observed that there is an increase in the EQE at wavelengths between 360 nm and 720 nm for Cells D in comparison to Cells C. The EQE of Cells D with a thin LiF layer is increased up to 60%, which exhibits

Table 1: Key photovoltaic parameters for the PSCs with various anode buffer layers under illumination 100 mW/cm^2 AM 1.5 G simulated solar light.

Samples	V_{oc} (V)	J_{sc} (mA/cm^2)	FF (%)	Best PCE (%)	*Ave. PCE (%)	R_s (Ω cm^2)	R_{sh} (Ω cm^2)
Cells A	0.61	6.0	19.3	0.71	0.63 ± 0.08	177.1	95.7
Cells B	0.64	8.96	29.5	1.69	1.66 ± 0.03	115.5	284.0
Cells C	0.73	11.98	44.5	3.89	3.82 ± 0.07	36.2	321.6
Cells D	0.73	13.70	49.1	4.91	4.86 ± 0.05	20.1	381.9

*Average PCE: more than 30 cells were evaluated.

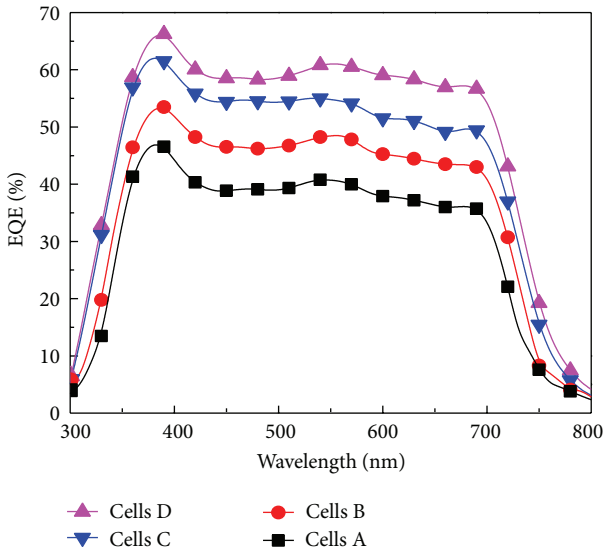

Figure 4: The EQE spectra of PSCs with various anode buffer layers.

efficient photon-to-electron conversion. The EQE spectra of PSCs also demonstrate that PEDOT:PSS/LiF as anode buffer layer could play positive effect on charge carrier collection. The adopting appropriate interfacial layers may provide an effective method to improve the performance of PSCs.

4. Conclusions

In summary, a series of PSCs based on PBDTTT-C and $PC_{71}BM$ as active layer were fabricated to investigate the anode buffer layers on the performance of PSCs. The performance of PSCs with PEDOT:PSS/LiF as anode buffer layer was improved compared with the cells fabricated on bare ITO substrates, LiF/ITO substrates, and PEDOT:PSS/ITO substrates. Cells D maintain a maximum J_{sc} and FF, yielding a highest PCE of 4.91%, which has a 26.2% improvement compared to the cells with PEDOT:PSS buffer layer. The improvement performance of PSCs can primarily be attributed to the efficient holes collection induced by the interfacial layer. The PEDOT:PSS/LiF anode buffer layer has positive effect on PSCs based on P3HT:PCBM system. These findings indicate that the optimization of anode buffer layer is an effective method for the improvement of PSCs.

Conflict of Interests

The authors declare that there is no conflict of interests regarding the publication of this paper.

Acknowledgments

This work was supported by Fundamental Research Funds for the Central Universities (2013JBZ004); National Natural Science Foundation of China (61377029); Beijing Natural Science Foundation (2122050); and the State Key Laboratory of Catalysis, CAS (n-11-09).

References

[1] W. Tang, J. Hai, Y. Dai et al., "Recent development of conjugated oligomers for high-efficiency bulk-heterojunction solar cells," *Solar Energy Materials and Solar Cells*, vol. 94, no. 12, pp. 1963–1979, 2010.

[2] L. Bian, E. Zhu, J. Tang, W. Tang, and F. Zhang, "Recent progress in the design of narrow bandgap conjugated polymers for high-efficiency organic solar cells," *Progress in Polymer Science*, vol. 37, no. 9, pp. 1292–1331, 2012.

[3] Z.-L. Zhuo, F.-J. Zhang, X.-W. Xu, J. Wang, L.-F. Lu, and Z. Xu, "Photovoltaic performance improvement of P3HT:PCBM polymer solar cells by annealing treatment," *Acta Physico-Chimica Sinica*, vol. 27, no. 4, pp. 875–880, 2011.

[4] D. W. Zhao, P. Liu, X. W. Sun, S. T. Tan, L. Ke, and A. K. K. Kyaw, "An inverted organic solar cell with an ultrathin Ca electron-transporting layer and MoO3 hole-transporting layer," *Applied Physics Letters*, vol. 95, no. 15, Article ID 153304, 2009.

[5] S.-I. Na, T.-S. Kim, S.-H. Oh, J. Kim, S.-S. Kim, and D.-Y. Kim, "Enhanced performance of inverted polymer solar cells with cathode interfacial tuning via water-soluble polyfluorenes," *Applied Physics Letters*, vol. 97, no. 22, Article ID 223305, 2010.

[6] Z. He, C. Zhong, X. Huang et al., "Simultaneous enhancement of open-circuit voltage, short-circuit current density, and fill factor in polymer solar cells," *Advanced Materials*, vol. 23, no. 40, pp. 4636–4643, 2011.

[7] J. Gao, C. L. Perkins, J. M. Luther et al., "N-type transition metal oxide as a hole extraction layer in PbS quantum dot solar cells," *Nano Letters*, vol. 11, no. 8, pp. 3263–3266, 2011.

[8] C. J. Brabec, S. E. Shaheen, C. Winder, N. S. Sariciftci, and P. Denk, "Effect of LiF/metal electrodes on the performance of plastic solar cells," *Applied Physics Letters*, vol. 80, no. 7, pp. 1288–1290, 2002.

[9] H. Wang, P. Amsalem, G. Heimel, I. Salzmann, N. Koch, and M. Oehzelt, "Band-bending in organic semiconductors: the role of alkali-halide interlayers," *Advanced Materials*, vol. 26, no. 6, pp. 925–930, 2014.

[10] M. G. Helander, Z. B. Wang, and Z. H. Lu, "Metal/fullerene electrode structure: physics and device applications," in *Organic Light Emitting Materials and Devices XII*, vol. 7051 of *Proceedings of SPIE*, San Diego, Calif, USA, August 2008.

[11] H. Xu, L.-Y. Yang, H. Tian, S.-G. Yin, and F.-L. Zhang, "Rhenium oxide as the interfacial buffer layer for polymer photovoltaic cells," *Optoelectronics Letters*, vol. 6, no. 3, pp. 176–178, 2010.

[12] F. Zhang, X. Xu, W. Tang et al., "Recent development of the inverted configuration organic solar cells," *Solar Energy Materials and Solar Cells*, vol. 95, no. 7, pp. 1785–1799, 2011.

[13] Y. Liu, F. J. Zhang, H. D. Dai et al., "Interfacial layer for efficiency improvement of solution-processed small molecular solar cells," *Solar Energy Materials and Solar Cells*, vol. 118, pp. 135–140, 2013.

[14] F. J. Zhang, D. W. Zhao, Z. L. Zhuo, H. Wang, Z. Xu, and Y. S. Wang, "Inverted small molecule organic solar cells with Ca modified ITO as cathode and MoO3 modified Ag as anode," *Solar Energy Materials and Solar Cells*, vol. 94, no. 12, pp. 2416–2421, 2010.

[15] D. W. Zhao, S. T. Tan, L. Ke et al., "Optimization of an inverted organic solar cell," *Solar Energy Materials and Solar Cells*, vol. 94, no. 6, pp. 985–991, 2010.

[16] S. B. Lee, J. Ho Beak, B. H. Kang et al., "The annealing effects of tungsten oxide interlayer based on organic photovoltaic cells," *Solar Energy Materials and Solar Cells*, vol. 117, pp. 203–208, 2013.

[17] M. T. Greiner, L. Chai, M. G. Helander, W.-M. Tang, and Z.-H. Lu, "Transition metal oxide work functions: the influence of cation oxidation state and oxygen vacancies," *Advanced Functional Materials*, vol. 22, no. 21, pp. 4557–4568, 2012.

[18] L. Chen, P. Wang, F. Li, S. Yu, and Y. Chen, "Efficient bulk heterojunction polymer solar cells using PEDOT/PSS doped with solution-processed MoO3 as anode buffer layer," *Solar Energy Materials and Solar Cells*, vol. 102, pp. 66–70, 2012.

[19] J. H. Seo, D.-H. Kim, S.-H. Kwon et al., "High efficiency inorganic/organic hybrid tandem solar cells," *Advanced Materials*, vol. 24, no. 33, pp. 4523–4527, 2012.

[20] Z. Wang, F. Zhang, J. Wang et al., "Organic photovoltaic cells: novel organic semiconducting materials and molecular arrangement engineering," *Chinese Science Bulletin*, vol. 57, no. 32, pp. 4143–4152, 2012.

[21] X. Xi, Q. Meng, F. Li et al., "The characteristics of the small molecule organic solar cells with PEDOT:PSS/LiF double anode buffer layer system," *Solar Energy Materials and Solar Cells*, vol. 94, no. 3, pp. 623–628, 2010.

[22] K. H. Kim and H. J. Chang, "Effects of buffer layers on properties of bulk hetero junction flexible organic solar cells," *Ceramics International*, vol. 39, no. 1, pp. S605–S609, 2013.

[23] H. Ma, H.-L. Yip, F. Huang, and A. K.-Y. Jen, "Interface engineering for organic electronics," *Advanced Functional Materials*, vol. 20, no. 9, pp. 1371–1388, 2010.